Tissue engineering a fetal membrane

TISSUE ENGINEERING: Part A
Volume 18, Numbers 3 and 4, 2012

DOI: 10.1089/ten.tea.2011.0194

Tissue Engineering a Fetal Membrane

Shengli Mi, Ph.D.,[1,2] Anna L. David, M.D.,[3] Bipasha Chowdhury, M.D.,[3] Roanne Razalia Jones, B.Sc.,[1] Ian William Hamley, Ph.D.,[1] Adam M. Squires, Ph.D.,[1] and Che John Connon, Ph.D.[1]

The aim of this study was to construct an artificial fetal membrane (FM) by combination of human amniotic epithelial stem cells (hAESCs) and a mechanically enhanced collagen scaffold containing encapsulated human amniotic stromal fibroblasts (hASFs). Such a tissue-engineered FM may have the potential to plug structural defects in the amniotic sac after antenatal interventions, or to prevent preterm premature rupture of the FM. The hAESCs and hASFs were isolated from human fetal amniotic membrane (AM). Magnetic cell sorting was used to enrich the hAESCs by positive ATP-binding cassette G2 selection. We investigated the use of a laminin/fibronectin (1:1)-coated compressed collagen gel as a novel scaffold to support the growth of hAESCs. A type I collagen gel was dehydrated to form a material mimicking the mechanical properties and ultra-structure of human AM. hAESCs successfully adhered to and formed a monolayer upon the biomimetic collagen scaffold. The resulting artificial membrane shared a high degree of similarity in cell morphology, protein expression profiles, and structure to normal fetal AM. This study provides the first line of evidence that a compacted collagen gel containing hASFs could adequately support hAESCs adhesion and differentiation to a degree that is comparable to the normal human fetal AM in terms of structure and maintenance of cell phenotype.

Introduction

The leading cause of perinatal and neonatal mortality is preterm birth, of which 40% is attributed to the preterm premature rupture of the membranes (pPROM).[1,2] pPROM occurs commonly when there is preterm funneling of the cervix with associated cervical dilation. Preventive therapies such as progesterone or cervical cerclage are available for women at high risk of preterm birth,[3] but most preterm deliveries occur in women considered to be at low risk. Interventions during pregnancy such as amniocentesis or chorionic villus sampling and fetoscopy, in particular, are associated with a high incidence of pPROM due to disruption to the integrity of the fetal amniotic membrane (AM) at the insertion site of the fetoscope.[4] A number of techniques such as plugging the insertion site with a silicon seal or with platelets have been developed to seal off the membrane defect after fetoscopy, but none have proved to be of much benefit.[5]

AM consists of a single layer of epithelial cells on a thick basement membrane that lies upon layers of collagenous tissue interspersed with mesenchymal cells. Interstitial collagens (mostly type I) predominate and maintain the mechanical integrity of the AM.[6] Cells from the human AM are of great interest as a source of cells for regenerative medicine because of their phenotypic plasticity.[7,8] Evidence in support of human amniotic epithelial cell (hAEC) pluripotency includes work by Sakuragawa *et al.*, who identified neural and glial markers on cultured hAECs.[9] Later studies reported that cultured hAECs synthesize and release acetylcholine, catecholamines,[10–12] and dopamine.[13,14] Hepatic differentiation of hAECs was also reported.[15] Alongside the plasticity of these cells, another advantage in the use of placental tissue for regenerative medicine is that it is readily available and easily procured without invasive procedures, and its use does not elicit ethics debate, avoiding the current controversies associated with the use of human embryonic stem cells.[16] These advantages have been put to effect previously, and isolated AM epithelial cells, keratinocytes, fibroblasts, and lung carcinoma cells have each been successfully expanded on the surface of substrates formed from decellularized AM[17–19] or polyesterurethane.[20] However, the aim of this study was to construct an artificial AM by combination of hAESCs and a compacted collagen scaffold that actually contained human amniotic stromal fibroblasts (hASFs), thereby closely mimicking the natural AM physiology. This artificial AM may have the potential to plug defects in the AM after antenatal interventions, or to prevent pPROM when there is funneling and dilatation of the cervix.

Materials and Methods

Isolation and enrichment of hAESCs

The placenta and fetal membranes (FMs) were collected under sterile conditions from healthy donor pregnant

[1]School of Chemistry, Food, and Pharmacy, University of Reading, Reading, United Kingdom.
[2]Shaanxi Institute of Ophthalmology, Xi'an, People's Republic of China.
[3]Institute for Women's Health, University College London, London, United Kingdom.

women undergoing delivery by elective term caesarean section at University College London Hospital (UCLH), United Kingdom ($n=8$). All donors gave written informed consent before tissue collection. This study was approved by the Joint University College London/UCLH Committees on the Ethics of Human Research. The amnion layer was prepared according to the methods previously described by Akle *et al.*[21,22] Amniotic and chorionic tissues were separated manually by blunt dissection and were washed briefly several times with chilled phosphate-buffered saline (PBS) without calcium and magnesium to remove blood. To release epithelial cells, the amnion membrane was incubated at 37°C with 0.05% trypsin (Invitrogen). The cells from the first 30 min of digestion were discarded to exclude debris. The cells from the second and third 30-min digests were pooled and washed three times with PBS. Cells collected by filtration (70 μm nylon mesh; Fisher brand) and centrifugation at 1500 *g* for 5 min were designated as hAECs.

Magnetic-activated cell sorting (MACS) was used to enrich the hAESCs by positive selection of ATP-binding cassette G2 (ABCG2), a marker of hAESCs.[22,23] In brief, after calculating the total epithelial cell number, the cells were incubated overnight at 4°C with primary antibody against ABCG2 (1:100; Millipore). The cells were then labeled with anti-mouse IgG microbeads (Miltenyi Biotec), washed again, and then applied as a cell suspension to a magnetic separator (Miltenyi Biotec). Isolated ABCG2-positive cells were designated as hAESCs, and subsequently used in all cell culture experiments. To assay the clone-forming efficiency, the ABCG2-positive cells and ABCG2-negative cells were seeded in a six-well plate at a density of 5000 cells/well. After 5 days of growth, cells were fixed in methanol for 15 min at room temperature and then stained with Giemsa for 30 min, washed with distilled water, and air-dried, before examining under an inverted microscope.

Isolation of hASFs

After removal of epithelial cells, the denuded AM (dAM) was subjected to a full mechanical and enzymatic digestion.[24] Pieces of dAM were gently minced in a controlled fashion by automated tissue dissociation (Miltenyi Biotec) and were subjected to enzymatic digestion using 0.25% trypsin–EDTA and 0.1% type I collagenase in Dulbecco's modified Eagle's medium (DMEM; Invitrogen) for 45 min at 37°C on a rotator until digestion was complete. The supernatant was neutralized with 5% fetal bovine serum (FBS; Sigma-Aldrich) in DMEM. The cells were centrifuged and then re-suspended in DMEM with 10% FBS in a humidified 5% CO_2 incubator at 37°C until they were 70% confluent using a 75 cm^2 tissue culture flask (Fisher). The expanded cells were collected and designated as hASFs.

Expansion of hAESCs on differently coated compacted collagen scaffolds embedded with amniotic stromal fibroblasts

Collagen gels were made as described previously[25] with some modifications. Briefly, collagen gels were prepared by 1 M sodium hydroxide (Fisher) neutralization of 4 mL of sterile rat-tail type I collagen (2.05 mg/mL; First Link) mixed with 0.5 mL of 10× minimum essential medium (Invitrogen). After neutralization, 0.5 mL of media containing hASFs was added at a concentration of 2.0×10^5 cells/mL, and the solution was gently mixed together and left on ice for 30 min before casting to prevent gelling while allowing dispersion of any small bubbles within the solution. The gel was cast into rectangular molds (33 mm × 21 mm × 8 mm) and set at 37°C, 0.5% CO_2 for 30 min. After the initial setting of the gels, they were then subsequently compacted by a combination of compression and dehydration. Each gel was sandwiched between layers of nylon and metal mesh and was then compressed by applying a weight of 120 g for 5 min at room temperature, leading to the formation of a flat collagen sheet embedded with viable hASFs. The largest pore size (gaps between collagen fibers) between compressed collagen gel and dAM were analyzed by Axiovision Rel.4.8 software (Carl Zeiss Microimaging).

The resulting compacted collagen gels were then transferred into six-well plates (transwells; Costar) and each gel was coated with fibronectin (2.5 μg/cm^2; Sigma-Aldrich), collagen IV (8 μg/cm^2; Sigma-Aldrich), laminin (1.5 μg/cm^2; Sigma-Aldrich), or fibronectin/laminin (1:1; Sigma-Aldrich), which were diluted with PBS, respectively. The scaffolds were incubated at 37°C for 2 h and washed three times with PBS. MACS-enriched hAESCs were then plated on the differently coated collagen gels within a 24-mm-diameter transwell at a density of 1×10^6 cells per cm^2 in our standard culture medium (DMEM supplemented with 10% FBS, 10 ng/mL epidermal growth factor, 2 mM L-glutamine, 1% nonessential amino acid, 1 mM sodium pyruvate, and 1% antibiotic–antimycotic; all from Invitrogen). The cell attachment efficiency was measured on the differently coated collagen scaffolds. Cells were allowed to attach to the scaffolds overnight, and before the first round of cell division, the unattached cells were collected by gentle washing and counted using a hemocytometer. The cell attachment efficiency was calculated as the number of attached cells remaining as compared with the total number of cells originally plated on the scaffold.

Rheology of scaffolds

The mechanical properties of compacted collagen gels (with encapsulated hASFs) and dAM were compared using a controlled stress AR-2000 rheometer (TA Instruments). A cone-and-plate geometry (cone diameter 20 mm, angle 1) was used for all samples. Preliminary oscillatory stress sweeps were performed at a fixed frequency of 1 Hz between 0.1 and 100 Pa at 37°C to ensure that the moduli were independent of stress. After this, frequency sweeps were performed with the machine in oscillatory mode at an angular frequency range (ω) of 0.1–100 rad/s under a controlled stress of 5 Pa.

Electron microscopy

dAM, compacted collagen gel with embedded hASFs, normal AM, and our fully constructed artificial AM were examined by scanning electron microscopy (SEM). The normal AM and constructed artificial AM were examined by transmission electron microscopy (TEM). Specimens were fixed in 2.5% (v/v) glutaraldehyde, and postfixed for 2 h in 1% aqueous osmium tetroxide. They were then washed with distilled water before being passed through a graded ethanol series. For SEM, specimens were transferred to

hexamethyldisilazane for 20 min and allowed to air-dry. These specimens were then mounted on aluminum stubs and sputter coated with gold before examination using an SEM (FEI Quanta FEG 600). For TEM, the dehydrated specimens were embedded in epoxy resin (Agar 100; Agar Scientific, Ltd.). Ultrathin (70 nm) sections were collected on copper grids and stained for 1 h with uranyl acetate and 1% phosphotungstic acid, and then for 20 min with Reynolds' lead citrate before examination using a transmission electron microscope (Philips CM20).

Hematoxylin and eosin staining

Normal AM and our fully constructed artificial AM were examined by hematoxylin and eosin (H&E) staining. Cryosections (5 μm thick) were routinely processed and examined by light microscopy after H&E staining.

Immunohistochemistry

Normal AM and the artificial AM were examined by immunofluorescence. Both tissues were treated with 1% bovine serum albumin in 50 mM Tris-buffered saline (pH 7.2), containing 0.4% Triton X-100 for 60 min at room temperature. Samples were then incubated overnight at 4°C with primary antibodies against ABCG2 (1:100; Millipore) and cytokeratin 19 (CK19, 1:100; Millipore). FITC-labeled secondary antibodies (1:100; Vector Laboratories, Inc.) were used. Samples were costained with propidium iodide (Vector Laboratories, Inc.) and observed by fluorescence microscopy (Carl Zeiss Meditec).

Statistical analysis

A Student's *t*-test (unpaired) was performed to compare rheology results using Microsoft Excel. Results are presented as the mean of three individual experiments with standard error of mean and $p < 0.05$ was considered significant.

Results

Morphology of artificial scaffolds

Both the compacted collagen gel with embedded hASFs and dAM had similar translucency; however, the compacted collagen gel appeared more homogeneous (Fig. 1A) than the dAM (Fig. 1B). The SEM analyses demonstrated that the collagen fibers within the compacted collagen gel appeared dense with fiber diameter and fiber arrangement similar to the dAM (Fig. 1C, D). Comparing the relative pore sizes (gaps between collagen fibers), the compressed gel was similar to the dAM. When comparing surface areas of approximately 6000 μm^2 between the compressed scaffold and dAM (control), the largest pore sizes were determined to be 672 and 659 nm, respectively, indicating similar pore sizes (Fig. 1C, D).

Rheology of scaffolds

Oscillatory shear rheology was used to probe the dynamic mechanical properties of compacted collagen gel and dAM, where G' (storage modulus) and G'' (loss modulus) refer to the stiffness and viscoelastic properties of the materials. Stress sweeps indicated that the compacted collagen gel had

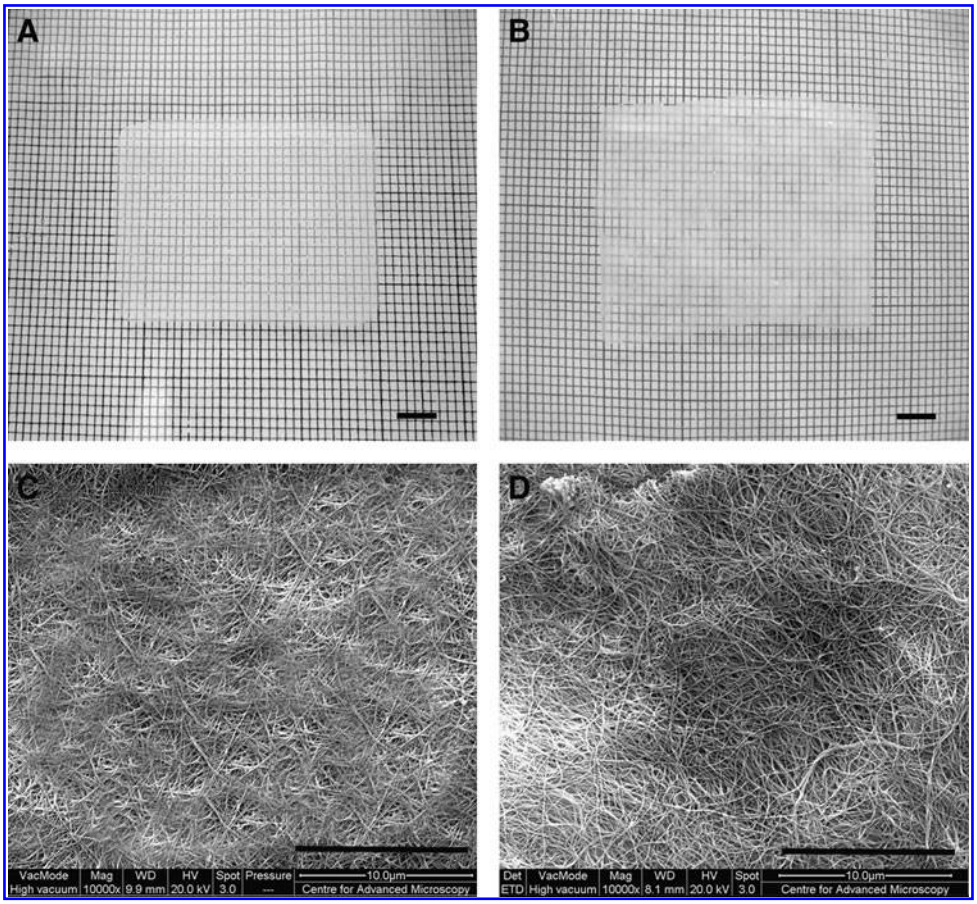

FIG. 1. **(A)** Compacted collagen gel embedded with human amniotic stromal fibroblasts (hASFs); **(B)** denuded amniotic membrane (dAM); scanning electron microscopy (SEM) of **(C)** compacted collagen scaffold surface and **(D)** dAM surface. Scale bar **(A, B)** 5 mm and **(C, D)** 10 μm.

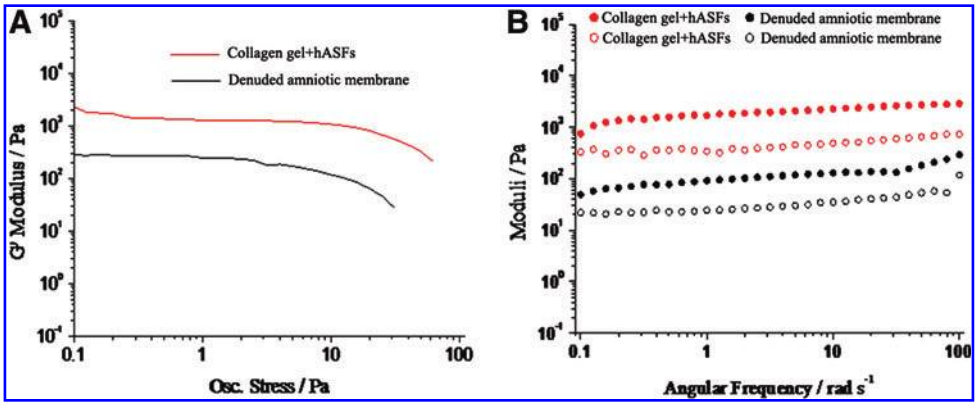

FIG. 2. The rheological properties of compacted collagen containing hASFs and dAM also containing native hASFs ($n=3$). Preliminary oscillatory stress sweeps carried out at 37°C **(A)**. Oscillatory frequency sweeps carried out at 37°C at a controlled stress of 5 Pa for both scaffolds. Closed and open circles refer to G' (storage modulus) and G'' (loss modulus), respectively **(B)**. Color images available online at www.liebertonline.com/tea

a longer linear regime than dAM and can withstand shearing at high stresses up to 25 Pa (Fig. 2A, $n=3$). Based on preliminary stress sweeps, a fixed stress of 5 Pa was selected for frequency sweep studies corresponding to stresses within the linear viscoelastic regime of both of our materials. Figure 2B showed the frequency sweep data for further characterization of the structure of our scaffolds ($n=3$). Both materials behaved as stiff gels with compacted collagen gel G' (2000 ± 51.67 Pa) $> 10^3$ and dAM G' (220 ± 101.39 Pa) $> 10^2$ at low frequencies. This indicated that compacted collagen gel is the stiffer of the two materials over a range of frequencies where G' remains constant ($p < 0.05$). The dynamic mechanical properties of both scaffolds appeared to demonstrate behavior of weak frequency dependence. In addition, values for G' are larger than G'' by a factor of 5–10 for both scaffolds, indicating an ordered structure.

MACS of amniotic epithelial cells

ABCG2 is recognized as a stem cell marker for hAESCs.[22,23] Expression of ABCG2 in primary hAESCs was evaluated by MACS using anti-ABCG2 micro-beads. ABCG2-positive cells accounted for 14% ($n=2$) of the cells in the primary hAEC population. A representative experiment is shown in Figure 3A and B. Colony-forming efficiency (CFE) was used to analyze the proliferation of the ABCG2-positive and -negative cell groups. The result indicated that the CFE of the ABCG2-positive group was demonstrably higher than that of the negative group (Fig. 3C, D).

Amniotic epithelial stem cells grown on coated compacted collagen gels with embedded hASFs

The hAESCs were cultured on noncoated (Fig. 4A), collagen IV (Fig. 4B), fibronectin (Fig. 4C), laminin (Fig. 4D), and fibronectin/laminin (1:1, Fig. 4E)-coated compacted collagen gels for 12 h, and the cell attachment efficiencies were found to be 17%, 61%, 69%, 66%, and 100%, respectively ($n=5$). The cells formed a continuous monolayer on the fibronectin/laminin (1:1)-coated collagen gel with a resulting ultrastructure similar to the normal AM control (Fig. 4F).

Morphology of hAESCs expanded upon compacted collagen gels with embedded hASFs

The morphology of hAESCs on fibronectin/laminin (1:1)-coated compacted collagen gel containing hASFs was studied on day 5 after high-density cell seeding. hAESCs exhibited a typical polygon-type cell shape with plenty of microvilli on the cell surface and formed a continuous monolayer on the compacted collagen gel (Fig. 5A) similar to normal AM (Fig. 5B).

H&E staining

Histological analysis using H&E staining showed that the tissue-engineered sheet formed a single continuous epithelial cell layer on the compacted collagen gel (Fig. 6A). This is similar to the epithelial structure of native AM (Fig. 6B). The hASFs that were encapsulated in the collagen scaffolds had a similar cell distribution pattern and cell density to the normal AM stroma, and the thickness of the artificial AM was also similar to the normal AM.

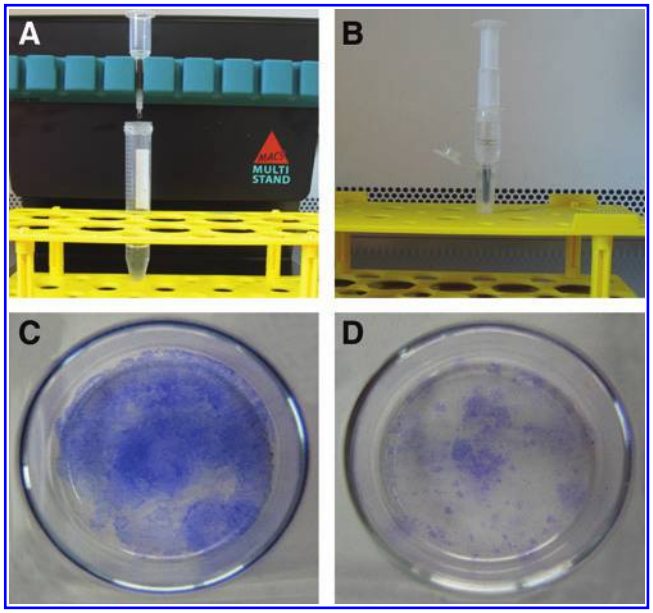

FIG. 3. Magnetically activated cell sorting to enrich human amniotic epithelial stem cells (hAESCs) **(A)**. ABCG2-negative cells flow through the column and ABCG2-positive cells adhered on the column. The ABCG2-positive cells were flushed out by firmly pushing the plunger into the column after removing the magnets **(B)**. The colony-forming efficiency of ABCG2-positive cell group **(C)** and ABCG2-negative cell group **(D)**. Color images available online at www.liebert online.com/tea

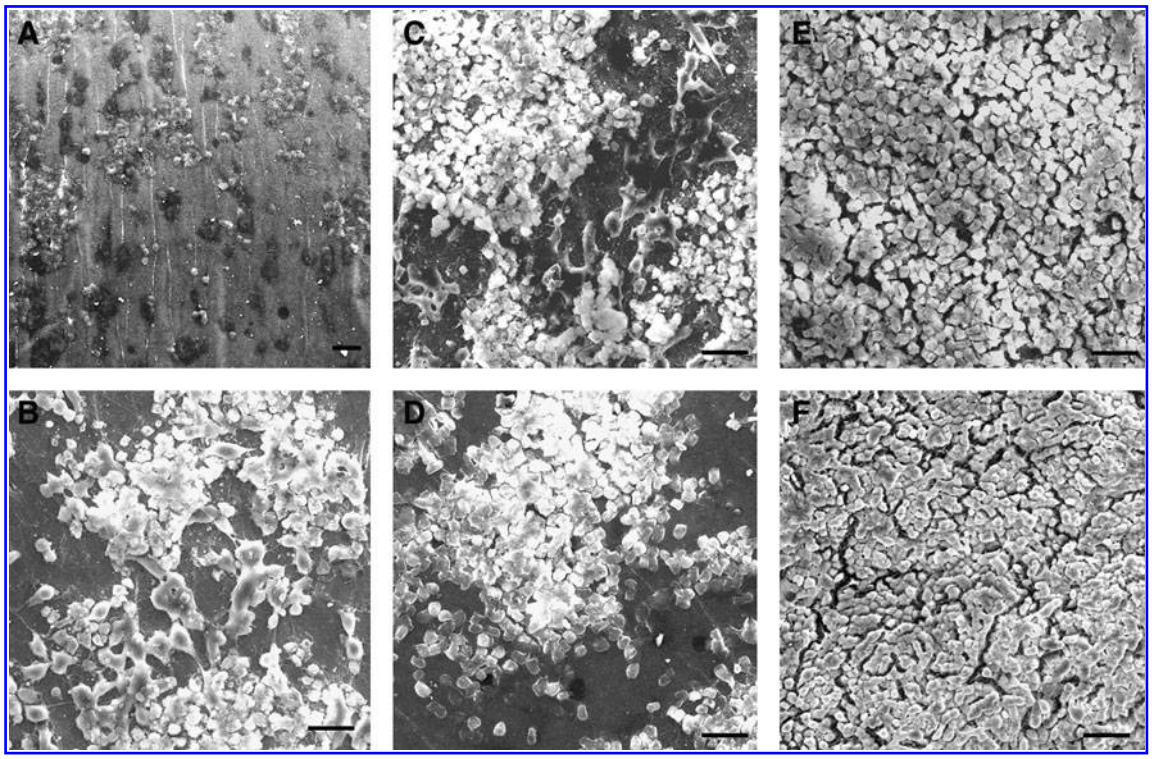

FIG. 4. hAESCs cultured on noncoated **(A)**, collagen IV-coated **(B)**, fibronectin-coated **(C)**, laminin-coated **(D)**, and fibronectin/laminin (1:1)-coated **(E)** compressed gels. **(F)** normal AM. Scale bar = 50 μm.

Transmission electron microscopy

TEM analyses indicated that the hAESCs expanded upon the compacted collagen gel had produced a defined basement membrane with evidence of hemidesmosome formation on the basal side (Fig. 7A), and neighboring cells were attached via desmosome structures (Fig. 7B).

Immunohistochemistry

After culture for 5 days, the hAESCs were distributed evenly on the scaffold and formed a monolayer. ABCG2, a marker of hAESCs,[22,23] was expressed in the membrane of cells from both artificial AM (Fig. 8A–C) and normal AM (Fig. 8G–I). Another hAESC marker, CK19, was expressed in the cytoplasm of epithelial cells from artificial AM (Fig. 8D–F) and normal AM (Fig. 8J–L). Compared with the artificial AM, the normal AM epithelial cells had a higher proportion of ABCG2- and CK19-positive cells (see the merged color images [Fig. 8 C, F, I, L] for CK19 [green; Fig. 8B, E, H, K], and propidium iodide [red; Fig. 8A, D, G, J], respectively].

Discussion

This study demonstrates the successful *ex vivo* construction of an FM by combination of human amniotic stem cells and a compacted collagen gel containing human amniotic fibroblasts. The resulting cellular–collagen construct displays many of the structural and functional properties of human AM.

The hAESCs represent an important source of cells with pluripotential characteristics.[22,26] Preclinical and clinical

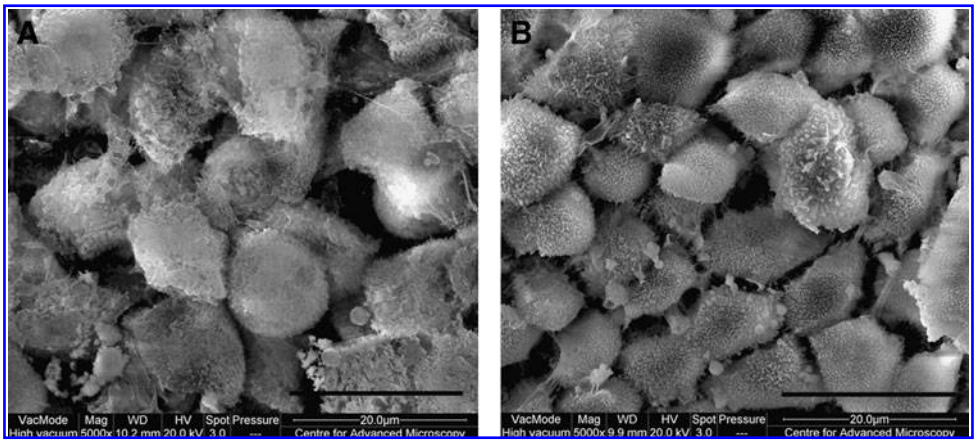

FIG. 5. SEM of hAESCs grown on fibronectin/laminin (1:1)-coated compressed collagen scaffold **(A)**. Control normal human AM epithelial cells **(B)**. Scale bar = 20 μm.

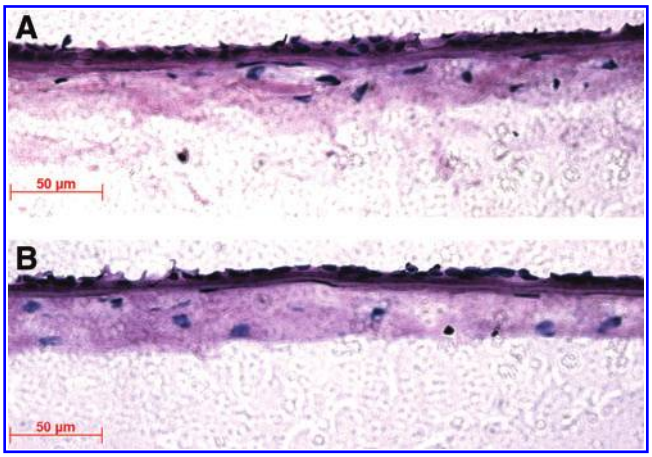

FIG. 6. Hematoxylin and eosin staining of tissue-engineered human AM **(A)** and normal (native) human AM **(B)**. Scale bar = 50 μm. Color images available online at www.liebertonline.com/tea

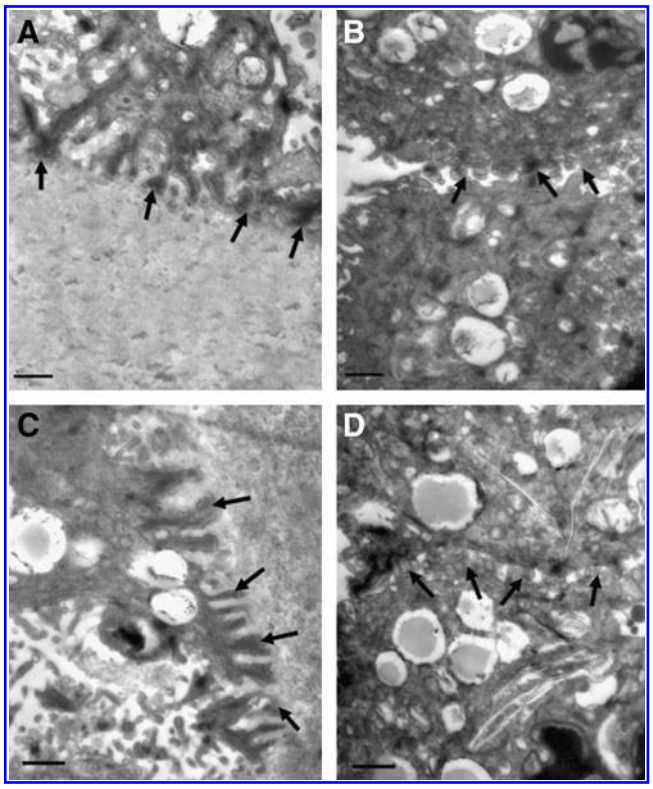

FIG. 7. Transmission electron microscopy images of tissue engineering AM and normal AM. **(A)** Basal cells appeared to adhere well to the compressed collagen scaffold via hemidesmosome attachments (arrows). **(B)** Neighboring cells displayed desmosome junctions (arrows). **(C)** Hemidesmosome attachments in normal AM (arrows). **(D)** Desmosome junctions in normal AM (arrows). Scale bars = 1 μm.

studies have demonstrated high proliferation ability and multiple uses for hAESCs in tissue repair, such as corneal tissue,[27] spinal cord injury,[28] brain infarction,[10] and Parkinson's disease.[14] In this study, we used a MACS method to enrich the hAESCs by positive selection of ABCG2,[22,23] the CFE of ABCG2-positive cells was much higher than that of ABCG2-negative cells, indicating that the enriched positive cells have strong proliferative ability, one common property of stem cells.

Cell adhesion to a material is mediated primarily by the interaction between surface bound proteins and the corresponding receptors on the cell membrane.[29] Extensive research on the cellular response to different proteins preadsorbed onto various surfaces, including collagen,[30,31] laminin,[32,33] and fibronectin,[34,35] indicates that synthetic materials must adsorb proteins to improve their interaction with cells.[36–38] Amniotic epithelial cells are easily detached from the amniotic stroma to float in the amniotic fluid. Therefore, in this study, we investigated the adhesion and growth of primary hAESCs on compacted collagen gels coated with collagen IV, fibronectin, or laminin to improve epithelial cell adhesion and spreading. Our results showed that substrate surfaces coated with collagen IV, laminin, or fibrnoectin did not achieve hAESC confluence; nevertheless, growth was significantly enhanced compared to hAESCs cultured on a plain collagen type I surface. Importantly, however, hAESCs cultured on a combined laminin/fibronectin (1:1)-coated surface were able to grow to confluence, producing a tissue very similar in structure to the normal AM. The reason for this may be that the presence of the two kinds of coated proteins (laminin/fibronectin) increased surface-bound protein expression in response to corresponding cell receptors, and once the cells adhere, they generated their own extracellular matrix, creating an optimal environment for their survival.[39]

Although we were successful in maintaining a population of ABCG2-positive hAESCs on the compressed collagen gel *ex vivo* and that this level may be therapeutically relevant, a high proportion of cells did appear to lose ABCG2 expression in culture. We believe that this loss may in part be explained by the higher stiffness of the collagen gel compared to AM. Recently, several notable studies have demonstrated the importance of substrate stiffness in the regulation of stem cell differentiation.[40–42] Further, we have recently shown that a variation in either AM or compressed collagen gel stiffness could dramatically influence the differentiation of unipotent stem cells.[43,44] We believe that we are seeing the same phenomenon with hAESCs. However, in terms of its intended function, the creation of an artificial AM with a greater ability to store applied mechanical energy is also likely to be important.

We improved the mechanical properties of conventional collagen gels by compaction, resulting in a dense and mechanically strong collagen scaffold.[45] Similar to the results attained using compacted collagen gels containing corneal fibroblasts,[46] dehydration of the collagen gel maintained the viability of the encapsulated hASFs.[46] The SEM analyses demonstrated that the collagen fibers within the compacted gel appeared dense and homogeneous, and the fiber's diameter, arrangement, and the gel's relative pore size were similar to normal dAM. Subsequently, we successfully used this hASF-embedded, laminin/fibronectin (1:1)-coated compacted collagen gel as a novel substrate/scaffold to support the adherence and expansion of hAESCs—that is, a tissue-engineered human FM.

To achieve lasting closure of FM lesions, biomaterials are required that permit not only instant sealing of the

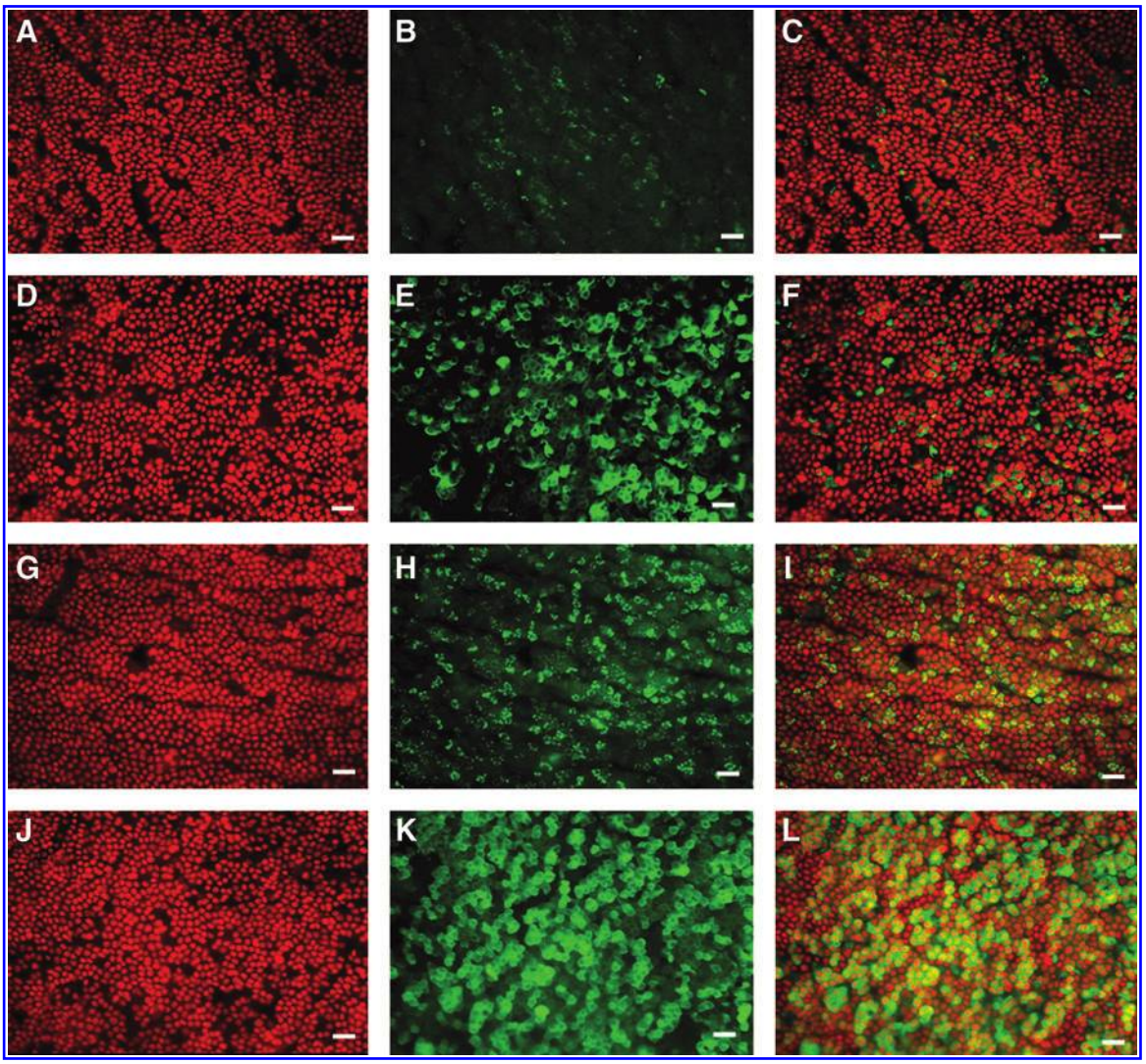

FIG. 8. Immunofluorescent staining for the hAESC markers ABCG2, CK19, and propidium iodide costained nuclei. Artificial AM stained for ABCG2 [see the merged color images **(C)** for ABCG2 **(**green; **B)** and propidium iodide **(**red; **A)**] and CK19 [see the merged color images **(I)** for CK19 **(**green; **H)** and propidium iodide **(**red; **G)**]. Normal AM-stained ABCG2 [see the merged color images **(F)** for ABCG2 **(**green; **E)** and propidium iodide **(**red; **D)**] and CK19 [see the merged color images **(L)** for CK19 **(**green; **K)** and propidium iodide **(**red; **J)**]. Scale bar = 50 μm. Color images available online at www.liebertonline.com/tea

membrane leak but also subsequent anatomical repair of the lesion through recruited amnion cells. In the current study, we were able to replace decellularized AM with a finely regulated collagen gel that uniquely contained amniotic fibroblasts encapsulated within it. Using this engineered stroma, we explored whether the structural and functional properties required of the AM could be replicated and maintained by our tissue-engineered AM. In terms of the artificial AM for clinical use, possibly safety concerns could be addressed by replacing rat tail collagen with bovine (for which there is food and drug administration approval) or less-immunogenic sources of collagen such as collagen extracted from human placenta or recombinant human type I collagen. Our results showed that under culture conditions without other cell-derived feeder layers, hAESCs adhered to fibronectin-laminin (1:1)-coated compacted collagen scaffold, exhibiting a typical polygon-type cell shape with plenty of microvilli forming a confluent monolayer after culture for 1 week. Further, immunophenotypic characterization of hAESCs demonstrated expression of well-defined markers of hAESCs, that is, ABCG2[22,23] and CK19. H&E staining showed that both epithelial cells and stromal cells within the artificial AM had a similar cell distribution pattern, cell density, and thickness to normal AM.[47] The TEM images revealed that epithelial cells of artificial AM connected with collagen scaffold through hemidesmosome attachments and formed basal membrane, and the epithelial cells connected each other through desmosomes similar to normal AM.

Conclusions

This is the first study to describe the bottom up manufacture of a tissue-engineered FM using totally discrete components that significantly allow for the encapsulation of hASFs. Specifically, a combination of hAESCs and a fibronectin-laminin (1:1)-coated compacted collagen scaffold

containing hASFs was constructed *ex vivo*. The collagen scaffold was found to support the attachment of hAESCs and differentiation into amniotic epithelial cells. The artificial AM retained structural and functional properties similar to normal AM, and this human tissue construct may become a useful means to repair iatrogenic defects in the FMs or cases of pPROMs.

Acknowledgments

The authors thank Prof. Xiuping Zhu, Dr. Bo Chen, Dr. Bernice Wright, and Dr. Yun Feng for their support in experiments on isolation of AM epithelial cells. A.L.D. was supported by the UCL/UCLH Biomedical Research Centre, which is funded by the UK National Institute for Health Research. This study was financially supported by the Biotechnology and Biological Sciences Research Council of United Kingdom (Grant Ref: BB/F019742/1).

Disclosure Statement

No competing financial interests exist.

References

1. Penny, C.M., and Stephen, C.B. The fetal membranes and mechanisms underlying their labour-associated and prelabour rupture during pregnancy. Fetal Matern Med Rev **15,** 73, 2004.
2. Weisz, B., David, A.L., Chitty, L., Peebles, D., Pandya, P., Patel, P., and Rodeck, C.K. Association of isolated short femur in the mid-trimester fetus with perinatal outcome. Ultrasound Obstet Gynaecol **31,** 512, 2008.
3. Chandiramani, M., and Shennan, A.H. Preterm labour: update on prediction and prevention strategies. Curr Opin Obstet Gynecol **18,** 618, 2006.
4. Deprest, J., Lerut, T.E., and Vandenberghe, K. Operative fetoscopy: new perspective in fetal therapy? Prenat Diagn **17,** 1247, 1997.
5. Grozdana, B., Carrie, B., Phillip, B.M., Ajit, S.M., Thomas, M.Q., Claudia, H., Done, E., Gucciardo, L., Zeisberger, S.M., Zimmermann, R., Deprest, J., and Zisch, A.H. Injectable candidate sealants for fetal membrane repair: bonding and toxicity *in vitro*. Am J Obstet Gynecol **202,** e1, 2010.
6. Malak, T.M., Ockleford, C.D., Bell, S.C., Dalgleish, R., Bright, N., and Macvicar, J. Confocal immunofluorescence localization of collagen types I, III, IV, V and VI and their ultrastructural organization in term human fetal membranes. Placenta **14,** 385, 1993.
7. Parolini, O., Alviano, F., Bagnara, G.P., Bilic, G., Buhring, H.J., Evangelista, M., Hennerbichler, S., Liu, B., Magatti, M., Mao, N., Miki, T., Marongiu, F., Nakajima, H., Nikaido, T., Portmann, C.B., Sankar, V., Soncini, M., Stadler, G., Surbek, D., Takahashi, T.A., Redl, H., Sakuragawa, N., Wolbank, S., Zeisberger, S., Zisch, A., and Strom, S.C. Concise review: isolation and characterization of cells from human term placenta: outcome of the first international Workshop on Placenta Derived Stem Cells. Stem Cells **26,** 300, 2008.
8. Tamagawa, T., Ishiwata, I., and Saito, S. Establishment and characterization of a pluripotent stem cell line derived from human amniotic membranes and initiation of germ layers in vitro. Hum Cell **17,** 125, 2004.
9. Sakuragawa, N., Thangavel, R., Mizuguchi, M. Hirasawa, M., and Kamo, I. Expression of markers for both neuronal and glial cells in human amniotic epithelial cells. Neurosci Lett **209,** 9, 1996.
10. Sakuragawa, N., Misawa, H., Ohsugi, K., Kakishita, K., Ishii, T., Thangavel, R., Tohyama, J., Elwan, M., Yokoyama, Y., Okuda, O., Arai, H., Ogino, I., and Sato, K. Evidence for active acetylcholine metabolism in human amniotic epithelial cells: applicable to intracerebral allografting for neurologic disease. Neurosci Lett **232,** 53, 1997.
11. Elwan, M.A., and Sakuragawa, N. Evidence for synthesis and release of catecholamines by human amniotic epithelial cells. Neuroreport **8,** 3435, 1997.
12. Elwan, M.A., Thangavel, R., Ono, F., and Sakuragawa, N. Synthesis and release of catecholamines by cultured monkey amniotic epithelial cells. J Neurosci Res **53,** 107, 1998.
13. Kakishita, K., Elwan, M.A., Nakao, N., Itakura, T., and Sakuragawa, N. Human amniotic epithelial cells produce dopamine and survive after implantation into the striatum of a rat model of Parkinson's disease: a potential source of donor for transplantation therapy. Exp Neurol **165,** 27, 2000.
14. Kakishita, K., Nakao, N., Sakuragawa, N., and Itakura, T. Implantation of human amniotic epithelial cells prevents the degeneration of nigral dopamine neurons in rats with 6-hydroxydopamine lesions. Brain Res **980,** 48, 2003.
15. Sakuragawa, N., Enosawa, S., Ishii, T., Thangavel, R., Tashiro, T., Okuyama, T., and Suzuki, S. Human amniotic epithelial cells are promising transgene carriers for allogeneic cell transplantation into liver. J Hum Genet **45,** 171, 2000.
16. Toda, A., Okabe, M., Yoshida, T., and Nikaido, T. The potential of amniotic membrane/amnion - derived cells for regeneration of various tissues. J Pharmacol Sci **105,** 215, 2007.
17. Portmann, L.C.B., Ochsenbein, K.N., Marquardt, K., Luthi, U., Zisch, A., and Zimmermann, R. Manufacture of a cell-free amnion matrix scaffold that supports amnion cell outgrowth *in vitro*. Placenta **28,** 6, 2007.
18. Wilshaw, S.P., Kearney, J., Fisher, J., and Ingham, E. Biocompatibility and potential of acellular human amniotic membrane to support the attachment and proliferation of allogeneic cells. Tissue Eng Part A **14,** 463, 2008.
19. Wilshaw, S.P., Kearney, J.N., Fisher, J., and Ingham, E. Production of an acellular amniotic membrane matrix for use in tissue engineering. Tissue Eng **12,** 2117, 2006.
20. Ochsenbein, K.N., Jani, J., Lewi, L., Verbist, G., Vercruysse, L., Portmann, L.B., Marquardt, K., Zimmermann, R., and Deprest, J. Enhancing sealing of fetal membrane defects using tissue engineered native amniotic scaffolds in the rabbit model. Am J Obstet Gynecol **196,** e1, 2007.
21. Akle, C.A., Adinolfi, M., Welsh, K.I., Welsh, K.I., Leibowitz, S., and McColl, I. Immunogenicity of human amniotic epithelial cells after transplantation into volunteers. Lancet **2,** 1003, 1981.
22. Miki, T., Lehmann, T., Cai, H., Stolz, D.B., and Strom, S.C. Stem cell characteristics of amniotic epithelial cells. Stem Cell **23,** 1549, 2005.
23. Ilancheran, S., Moodley, Y., and Manuelpillai, U. Human fetal membranes: a source of stem cells for tissue regeneration and repair? Placenta **30,** 2, 2009.
24. Kita, K., Gauglitz, G.G., Phan, T.T., Herndon, D.N., and Jeschke, M.G. Isolation and characterization of mesenchymal stem cells from the sub-amniotic human umbilical cord lining membrane. Stem Cells **19,** 491, 2010.
25. Brown, R.A., Wiseman, M., Chuo, C.B., Cheema, U., and Nazhat, S.N. Ultrarapid engineering of biomimetic materials

and tissues: fabrication of nano- and microstructures by PC. Adv Funct Mater **15,** 1762, 2005.
26. Yen, B.L., Huang, H.I., Chien, C.C., Jui, H.Y., Ko, B.S., Yao, M., Shun, C.T., Yen, M.L., Lee, M.C., and Chen, Y.C. Isolation of multipotent cells from human term placenta. Stem Cells **23,** 3, 2005.
27. Shimmura, S., and Tsubota, K. Ocular surface reconstruction update. Curr Opin Ophthalmol **13,** 213, 2002.
28. Sankar, V., and Muthusamy, R. Role of human amniotic epithelial cell transplantation in spinal cord injury repair research. Neuroscience **118,** 11, 2003.
29. Norde, W., and Lyklema, J. Why proteins prefer interfaces. J Biomater Sci Polym Ed **2,** 183, 1991.
30. Thompson, K.P., Hanna, K.D., Gipson, I.K., Gravagna, P., Warring, G.O.I., and Johnson, W.B. Synthetic epikeratoplasty in rhesus monkeys with human type IV collagen. Cornea **12,** 35, 1993.
31. Kirkham, S.M., and Dangel, M.E. The keratoprosthesis: improved biocompatibility through design and surface modification. Ophthal Surg **22,** 455, 1991.
32. Grushkin, L.S., Kewalramani, R., and Trinkaus, R.V. Expression of integrin receptors on plasma membranes of primary corneal epithelial cells is matrix specific. Exp Eye Res **64,** 323, 1997.
33. Trinkaus, R.V., Vural, M., Capecchi, J., Franzblau, C., and Leibowitz, H.M. Modification of polymers for synthesis by corneal epithelial cells. Invest Ophthalmol Vis Sci **32,** 1072, 1991.
34. Groth, T., and Altankov, G. Studies on cell–biomaterial interaction: Role of tyrosine phosphorylation during fibroblast spreading on surfaces varying in wettability. Biomaterials **17,** 1227, 1996.
35. Pettit, D.K., Horbett, T.A., and Hoffman, A.S. Influence of the substrate binding characteristics of fibronectin on corneal epithelial cell outgrowth. J Biomed Mater Res **26,** 1259, 1992.
36. Altankov, G., and Groth, T.H. Reorganization of substratum-bound fibronectin on hydrophilic and hydrophobic materials is related to biocompatibility. J Mater Sci Mater Med **5,** 732, 1994.
37. Juliano, D.J., Saavedra, S.S., and Truskey, G.A. Effect of the conformation and orientation of adsorbed fibronectin on endothelial cell spreading and the strength of adhesion. J Biomed Mater Res **27,** 1103, 1993.
38. Grinnell, F., and Feld, M. Fibronectin adsorption on hydrophilic and hydrophobic surfaces detected by antibody binding and analyzed during cell adhesion in serum containing medium. J Biol Chem **257,** 4888, 1982.
39. Jacob, J.T., Rochefort, J.R., Bi, J., and Gebhardt, B.M. Corneal epithelial cell growth over tethered-protein/peptide surface-modified hydrogels. J Biomed Mater Res B **72,** 198, 2005.
40. Engler, A.J., Sen, S., Sweeney, H.L., and Discher, D.E. Matrix elasticity directs stem cell lineage specification. Cell **126,** 677, 2006.
41. Park, J.S., Chu, J.S., Tsou, A.D., Diop, R., Tang, Z., Wang, A., and Li, S. The effect of matrix stiffness on the differentiation of mesenchymal stem cells in response to TGF-β. Biomaterials **32,** 3921, 2011.
42. Levy, M.M., Zoldan, J., and Levenberg, S. Effect of scaffold stiffness on myoblast differentiation. Tissue Eng Part A **15,** 935, 2009.
43. Connon, C.J., and Chen, B. Location and structure of amniotic membrane affects the success of limbal stem cell expansion. ARVO Meet Abstr **52,** 3940, 2011.
44. Jones, R.R., Mi, S.L., Chen, B., Hamley, I.W., and Connon, C.J. Investigating the mechanical properties of collagen substrates and their influence on the *ex vivo* expansion of limbal epithelial cells. ARVO Meet Abstr **52,** 312, 2011.
45. Mi, S.L., Chen B., Wright, B., and Connon, C.J. Plastic compression of a collagen gel forms a much improved scaffold for ocular surface tissue engineering over conventional collagen gels. J Biomed Mater Res A **95,** 447, 2010.
46. Mi, S., Chen, B., Wright, B., and Connon, C.J. *Ex vivo* construction of an artificial ocular surface by combination of corneal limbal epithelial cells and a compressed collagen scaffold containing keratocytes. Tissue Eng Part A **16,** 2091, 2010.
47. Connon, C.J., Doutch, J., Chen, B., Hopkinson, A., Mehta, J.S., Nakamura, T., Kinoshita, S., and Meek, K.M. The variation in transparency of amniotic membrane used in ocular surface regeneration. Br J Ophthalmol **94,** 1057, 2010.

Address correspondence to:
Che John Connon, Ph.D.
School of Chemistry, Food and Pharmacy
Hopkins Building
University of Reading
Reading RG6 6UB
United Kingdom

E-mail: c.j.connon@reading.ac.uk

Received: April 4, 2011
Accepted: September 1, 2011
Online Publication Date: October 24, 2011